ION CHANNELS, RECEPTORS AND TRANSPORTERS

ClC-1 and ClC-2 form hetero-dimeric channels with novel protopore functions

Gabriel Stölting · Martin Fischer · Christoph Fahlke

Abstract CLC-type chloride channels exhibit a unique double-barreled architecture with two independently functioning ion conduction pathways, the so-called protopores. There exist gating processes that open and close individual protopores as well as common processes that jointly mediate slow opening and closing of both protopores. Different isoforms exhibit distinct voltage dependences and kinetics of gating. Whereas opening of the individual and common gate of homo-dimeric ClC-1 is promoted by membrane depolarization, ClC-2 is closed at positive potentials and opens only at negative voltages. To characterize the functional interaction of protopores we engineered a concatameric construct linking the coding regions of ClC-1 and ClC-2 in an open reading frame, expressed it in mammalian cells and measured anion currents through whole-cell and single channel patch clamping. In the hetero-dimeric assembly, each protopore displayed two kinetically distinct gating processes. Fast gating of the ClC-1 protopore closely resembled fast protopore gating of homo-dimeric channels. The voltage dependence of ClC-2 fast gating was shifted to more positive potentials by the adjacent ClC-1 protopore, resulting in open ClC-2 protopores at positive voltages. We observed two slow gating processes individually acting on ClC-1 and ClC-2 protopores, with distinct time and voltage dependences. Single channel recordings demonstrated that hetero-dimerization additionally modified the unitary conductance of ClC-2 protopores. Our findings suggest that inter-subunit interactions do not only affect common gating, but also ion permeation and gating of individual protopores in hetero-dimeric ClC channels.

Keywords CLC chloride channel · Single channel recording · Channel gating

Introduction

CLC-type chloride channels and chloride–proton exchangers exhibit a unique, evolutionarily conserved double-barreled architecture with two ion conduction pathways, each formed by a single subunit [10, 30]. This peculiar architecture is the basis of two structurally distinct gating processes: fast opening and closing of individual protopores as well as slow cooperative gating steps that act on both protopores together [30]. Whereas the molecular basis of protopore gating is rather well understood [2, 6, 11, 12, 19, 35], little is known about the interaction between subunits during cooperative gating.

One tool to study such interactions is the functional characterization of hetero-dimeric channels consisting of two functionally distinct CLC subunits [15, 26, 29, 42]. ClC-1 and ClC-2 chloride channels differ profoundly in the voltage dependence of fast and slow gating. Whereas fast and slow opening of ClC-1 is stimulated by membrane depolarization [2, 16, 17, 23], individual and common gates of ClC-2 open upon membrane hyperpolarization [9, 20, 39]. We here analyzed gating and permeation of ClC-1–ClC-2 hetero-dimeric channels using heterologous expression in mammalian cells and whole-cell and single channel patch clamp recordings. To ensure a homogenous population of hetero-dimeric channels we generated a concatameric expression construct linking one ClC-1 and one ClC-2 subunit in one open reading frame.

G. Stölting (✉) · C. Fahlke (✉)
Institute of Complex Systems-Zelluläre Biophysik (ICS-4),
Forschungszentrum Jülich, 52425 Jülich, Germany
e-mail: g.stoelting@fz-juelich.de
e-mail: c.fahlke@fz-juelich.de

M. Fischer
Institut für Neurophysiologie, Medizinische Hochschule Hannover,
30625 Hannover, Germany

ClC-1–ClC-2 hetero-dimer channels might also exist in native human cells. ClC-1 is the predominant chloride channel in adult skeletal muscle, and a recent study reports expression of ClC-1 also in the central nervous system [7]. Since ClC-2 is ubiquitously expressed and the spontaneous formation of hetero-dimeric channels was already demonstrated [28], ClC-1–ClC-2 hetero-dimers possibly assemble in both tissues under physiological conditions. This biophysical characterization might help understanding possible functional roles of such hetero-dimeric channels.

Methods

Construction of expression plasmids, mutagenesis, and heterologous expression

To generate an expression plasmid encoding concatenated ClC-1–ClC-2 dimers the coding region for human ClC-1 and human ClC-2 were linked via a covalent linker [14, 15] and subcloned in the pSVL vector [22]. We constructed expression plasmids for both orders of the two coding regions, pSVL–ClC-1–ClC-2 (Fig. 1) and pSVL–ClC-2–ClC-1. Expression of the ClC-2–ClC-1 construct resulted in currents that differ in time and voltage dependences from currents in cells expressing the ClC-1–ClC-2 hetero-concatamer in a deactivating component even without prior hyperpolarization (Supplemental Fig. 1). Single channel recordings, however, demonstrated channels with the same properties for either order of subunit concatenation. We therefore concluded that the expression of pSVL–ClC-2–ClC-1 resulted in the additional occurrence of homo-dimeric ClC-1 or ClC-2 channels (Supplemental text). Since expression of pSVL–ClC-1–ClC-2 appears to better constrain the formation of hetero-dimers than the reverse pSVL–ClC-2–ClC-1 we exclusively used pSVL–ClC-1–ClC-2 for analyzing functional properties of hetero-dimeric channels. Transient transfections in HEK293 cells were performed with 0.5–2 μg of plasmid DNA using Lipofectamine 2000 (Invitrogen, Carlsbad, CA, USA). For single channel experiments, ClC-1–ClC-2 concatameric constructs were subcloned into the pcDNA5/FRT/TO vector and stably transfected into Flp-In T-Rex 293 cells (Invitrogen, Carlsbad, CA, USA) as described [21]. Experiments on Flp-In T-Rex–ClC-1–ClC-2 cells were performed with or without induction using up to 1 μg/ml tetracycline [38].

Experiments on homo-dimeric ClC-1 were performed on HEK293T cells transiently expressing pSVL–hClC-1 whereas the characterization of homo-dimeric ClC-2 was performed on a stable cell line, generated by selecting Flp-In-T-Rex 293 cells (Invitrogen) transfected with pcDNA5/FRT/TO hClC-2 [20].
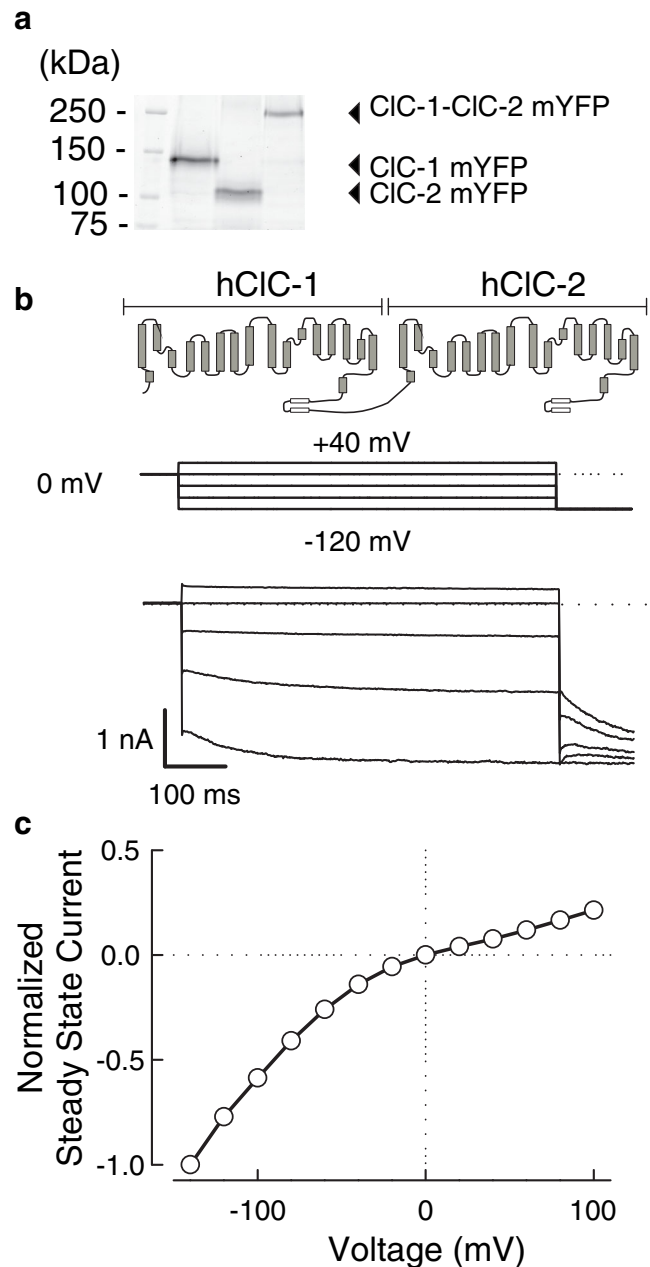
Fig. 1 Anion channels in cells expressing the ClC-1–ClC-2 concatamer show activation upon hyperpolarization and are active at positive potentials. **a** Fluorescence scan of an SDS-PAGE demonstrating expression of complete ClC-1–ClC-2 hetero-concatamers without visible formation of ClC monomers or proteolytic fragments. **b** Schematic representation of the ClC-1–ClC-2 hetero-dimer, pulse protocol, and representative current traces for ClC-1–ClC-2 hetero-dimeric channels expressed in HEK293T cells. **c** Normalized steady-state currents at voltage steps between −140 and +40 mV from cells ($n=5$) expressing ClC-1–ClC-2 hetero-dimeric channels, indicating open channels at positive potentials

Biochemical analysis

ClC-1, ClC-2, or ClC-1–ClC-2 was expressed in HEK293T cells as fusion proteins with yellow fluorescent protein (YFP) covalently linked to the carboxy-terminus of the channel proteins.

This method has been previously applied to homo-dimeric ClC-1 and ClC-2 without changes of biophysical properties [20, 22]. After lysis with 0.4 % n-dodecyl ß-D-maltoside in the presence of protease inhibitors (Roche Complete Cocktail, Roche Diagnostics Deutschland, Mannheim, Germany) cleared lysates were denatured for 15 min at 37 °C in SDS sample buffer containing 100 mM dithiothreitol. Samples were loaded on 8 % SDS polyacrylamide gels and run for approximately 1 h. Fluorescent samples and mass markers (Dual color; Bio-Rad, München, Germany) were visualized using a fluorescence scanner (Typhoon; GE Healthcare, München, Germany).

Whole-cell patch clamp and data analysis

Whole-cell patch clamp recordings were performed using an EPC10 amplifier (HEKA Elektronik, Lambrecht/Pfalz, Germany) as previously described [23, 38]. Standard solutions contained (in mM): NaCl (140), KCl (4), $CaCl_2$ (2), $MgCl_2$ (1), and HEPES (10) on the extracellular and (in mM): NaCl (115), $MgCl_2$ (2), EGTA (5), and HEPES (10) on the intracellular membrane side. To avoid contributions of endogenous potassium channels to whole-cell currents Na^+ was chosen as main internal cation instead of K^+. For experiments with variable $[Cl^-]$, Cl^- was substituted on an equimolar basis by gluconate. All solutions were adjusted to pH 7.4. The cells were clamped to 0 mV between test sweeps. Junction potentials were calculated using JPCalc (Dr. P. Barry, University of New South Wales, Sydney, Australia) and corrected for accordingly.

Data were analyzed using Pulse/Pulsefit (HEKA Elektronik; Lambrecht/Pfalz; Germany), pClamp (Molecular Devices, Sunnyvale, CA, USA) and SigmaPlot (Systat, San Jose, CA, USA). All values are given as mean ± SEM. Time constants of activation or deactivation were either obtained by fitting mono- or bi-exponential functions to the time dependence of current amplitudes [23] or of values obtained from envelope protocols [2]. Such protocols were used to determine slow activation time constants (Fig. 7) and consisted of a hyperpolarizing pulse of varying duration followed by a fixed 2 ms step to +200 mV and a following step back to the preceding potential were used. The duration of the voltage step to +200 mV was chosen to concur as closely as possible with the steady-state conditions of the ClC-1 fast gate without significantly affecting the other gates controlling the two protopores. Isochronal current amplitudes were determined 200 μs after a voltage step to +200 mV or to the subsequent negative voltage and plotted against the duration of the hyperpolarizing step. Monoexponential fits to the so-obtained time courses provided time constants of slow activation.

To obtain the voltage dependence of relative open probabilities of the protopore gates, isochronal current amplitudes were determined 200 μs after a voltage step to −120 mV following prepulses to various voltages, normalized by their maximum value, and plotted against the preceding potential. Unless otherwise stated, durations of the prepulses were adjusted to allow steady-state activation. To determine the voltage dependence of slow gate opening of ClC-2, a short pulse to −180 mV [9, 20] was inserted before the test step to −100 mV to fully activate the fast gate at this potential. The duration of this pulse was set to 15 ms as determined by extrapolation of the fast gate time constants in Fig. 6b to −180 mV. The relative open probabilities of the fast gate (Pf) were calculated by dividing the voltage dependence of the relative open probability (Po) by the open probability of the slow gate (Ps).

CLC channels are double-barreled, and the macroscopic ClC-1–ClC-2 currents thus consist of current components conducted by ClC-1 and ClC-2 protopores.

$$I_{\text{concatamer}} = I_{\text{ClC-1}} + I_{\text{ClC-2}} \tag{1}$$

Individual protopore currents ($I_{\text{protopore}}$) are given by the open probabilities of fast and slow gates open (P_{fast} and P_{slow}, respectively) multiplied by the number of channels (N) and the voltage-dependent single channel amplitude ($i(V)$).

$$I_{\text{protopore}} = N \cdot i(V) \cdot P_{\text{fast}}(V) \cdot P_{\text{slow}}(V) \tag{2}$$

To determine the open probability of the ClC-1 slow gate, we used a pulse protocol consisting of long pulses to various voltages that were interrupted by a fixed short step to +200 mV to activate the fast gate of ClC-1 (Fig. 5c). The current through the ClC-1 protopore preceding the short step to +200 mV is given by Eq. 2 while the instantaneous current following this jump is given by a modification of this equation:

$$I_{\text{ClC-1 instantaneous}} = N \cdot i(V) \cdot P_{\text{fast}}(+200 \text{ mV}) \cdot P_{\text{slow}}(V) \tag{3}$$

The fast gate of homo-dimeric ClC-1 is fully opened ($P_{\text{fast}} = 1$) [23] by a short depolarization to +200 mV. Although we could not determine absolute open probabilities of the ClC-1 protopore during such a short depolarization, due to the similar relative open probabilities and fast time constants of gating (Fig. 5) we assumed that the ClC-1 protopore within the hetero-dimeric assembly is opened to the same absolute value during the short depolarization regardless of the preceding voltage ($P_{\text{fast}} = $ constant). The deactivating current amplitude (ΔI) (Fig. 5c) therefore equals to:

$$\begin{aligned} \Delta I &= I_{\text{ClC-1 instantaneous}}(V) - I_{\text{ClC-1 late}}(V) \\ &= (N \cdot i(V) \cdot P_{\text{slow}}(V)) - (N \cdot i(V) \cdot P_{\text{fast}}(V) \cdot P_{\text{slow}}(V)) \end{aligned} \tag{4}$$

with N and $P_{\text{fast}}(+200 \text{ mV})$ being constant, the change in current is thus proportional to P_{slow}.

$$P_{\text{slow}} \sim \frac{\Delta I}{i(V) \cdot (1 - P_{\text{fast}}(V))} \tag{5}$$

Division of measured amplitudes by the known voltage-dependent conductance of homo-dimeric ClC-1 yields relative open probabilities [18].

For experiments with 9-anthracene carboxylic acid (9-AC; Sigma-Aldrich, Taufkirchen, Germany) [5] a 0.1-M stock solutions of 9-AC was prepared in DMSO. 9-AC was then dissolved in extracellular solution at concentrations of either 125 or 500 μM. The DMSO content of the final solution was kept below 0.1 %. The on- and offset of 9-AC block was recorded separately for the mean steady-state current or the amplitude of the hyperpolarization-dependent deactivation seen as in Fig. 2 and fit by mono-exponential functions. 9-AC is known to block ClC-1 channels by binding within the conduction pathway of each protopore separately [13]. Assuming a simple transition between an open, unbound state and a closed, 9-AC bound state, the determined time constants are defined as:

$$\tau_{on} = \frac{1}{k_{on}[9-AC] + k_{off}}$$
$$\tau_{off} = \frac{1}{k_{off}}$$

These equations were solved for the rate constants k_{on} and k_{off}, and the apparent dissociation constant was calculated as

$$k_D = \frac{k_{off}}{k_{on}}$$
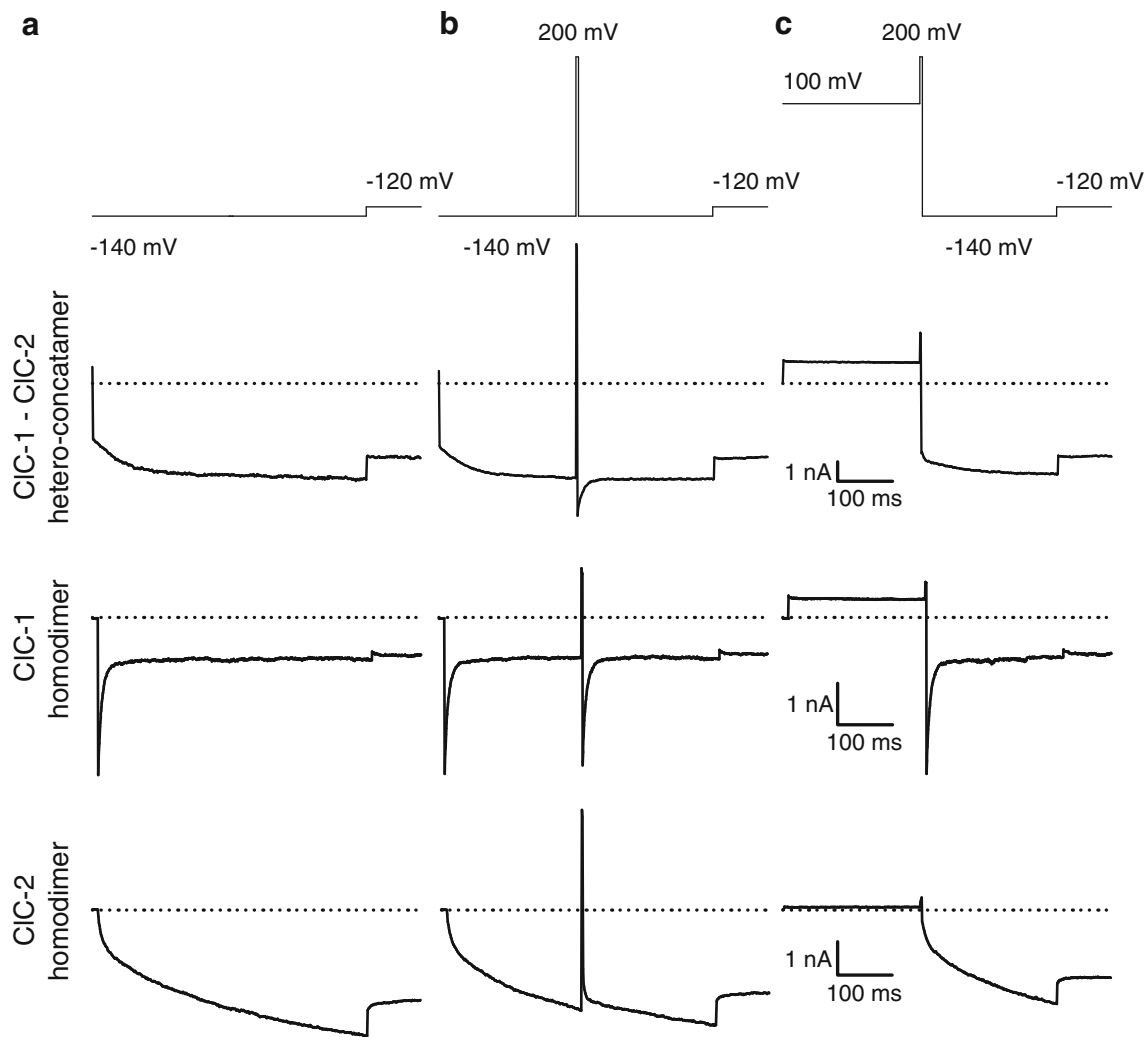
Fig. 2 Hetero-dimerization results in channels with novel gating properties. *a*, *b*, *c* Current responses of three representative cells expressing either ClC-1–ClC-2 concatameric channels, or homo-dimeric ClC-1 or ClC-2 to indicated pulse protocols

Noise analysis

We employed non-stationary noise analysis to determine unitary current amplitudes of homo-dimeric hClC-1 at positive potentials (Supplemental Fig. 2). For this, we initially determined the unitary current amplitude i and the number of channels at −155 mV as described previously [19, 41]. We then used the so determined number of channels (N) to calculate single channel amplitudes at other voltages by measuring the steady-state variance (σ^2) and mean macroscopic current (I) and solving the variance–current relationship taking previously published fast gate open probabilities (P_{fast}) [41] into account:

$$\sigma^2 = (1 + P_{\text{fast}}) \cdot i\langle I \rangle - \left(\frac{\langle I \rangle^2}{N} \right)$$

Single channel patch clamp and data analysis

Inside-out patches [38, 41] were drawn from Flp-In T-Rex 293 cells expressing ClC-1–ClC-2 hetero-concatamers. We used borosilicate pipettes with pipette resistances between 8 and 25 MΩ, and symmetrical bath and pipette solutions containing (in mM): NMDG·Cl (130), MgCl$_2$ (5), EGTA (5), and HEPES (10), adjusted to pH 7.4. Recordings were filtered using a 1 kHz Bessel filter. Analysis of single channel recordings was performed using the QuB Software (SUNY, Buffalo, NY, USA) after applying digital filtering at 300 Hz and a notch filter for the line frequency of 50 Hz. We chose 18 out of 194 successful inside-out patches for further analysis of the ClC-1–ClC-2 hetero-concatameric construct. The criteria for inclusion were recordings that were low unitary amplitude (all channels smaller than 1 pA at −100 or +100 mV) and sufficient stability throughout the recording. Out of these 18 patches, five could only be stably measured at −100 mV, eight at +100 mV, and five patches at both potentials. Statistical comparisons were performed in SigmaPlot (Systat, San Jose, CA, USA) using Student's t test.

Results

Expression of hetero-dimeric ClC-1–ClC-2 channels

We engineered a concatameric ClC-1–ClC-2 expression construct by covalently linking one ClC-1 and one ClC-2 coding sequence in a single reading frame using a short (20 amino acid) hydrophilic linker [15, 20, 22, 25, 37, 40, 41]. We first analyzed the concatameric ClC-1–ClC-2 expression construct after expression as YFP-fusion protein in mammalian cells. Reducing SDS-PAGE of the cell lysate (Fig. 1a) revealed a single band of the calculated size of the concatamer

(approximately 250 kD), without indication for the formation of monomers. Figure 1b shows representative current responses to voltages between −120 and +40 mV, each followed by a fixed step to −120 mV from a HEK293T cell expressing the concatameric construct. ClC-1–ClC-2 currents exhibit slow activation upon hyperpolarization and maintain a significant conductance at positive potentials (Fig. 1c). These properties differ from macroscopic currents conducted by homo-dimeric ClC-1 and ClC-2 since ClC-1 exhibits a strongly rectifying current voltage relationship [23, 34] whereas ClC-2 is closed at voltages positive to the chloride reversal potential and only slowly activates upon steps to negative potentials [20, 38].

Hetero-dimeric ClC-1–ClC-2 channels exhibit novel gating properties

Figure 2 shows current responses of ClC-1–ClC-2 as well as homo-dimeric ClC-1 and homo-dimeric ClC-2 to pulse protocols that were developed to separate fast and slow gating of ClC-1 and ClC-2 homo-dimers [2, 9, 20, 43]. Hetero-dimeric channels maintain a significant number of open channels at the holding potential of 0 mV and further activate upon prolonged membrane hyperpolarization (Fig. 2a). Homo-dimeric ClC-1 are deactivated upon such voltage steps whereas homo-dimeric ClC-2 activate on a slower time course with nearly zero open probability at 0 mV. We reasoned that the ClC-1 pore of hetero-dimeric channels might be closed at a holding potential of 0 mV and thus inserted a very short depolarization (10 ms) to +200 mV during the voltage step to −140 mV (Fig. 2b). This pulse protocol indeed elicited deactivating current component in cells expressing the hetero-concatamer. Homo-dimeric ClC-1 channels were activated by this short pulse, whereas homo-dimeric ClC-2 currents were only slightly modified by this short depolarization. Clamping the cells to +100 mV before the short step to +200 mV (Fig. 2c) did not result in such visible deactivation of ClC-1–ClC-2 hetero-concatamers. Homo-dimeric ClC-1 responded to these voltage steps with robust deactivation, whereas homo-dimeric ClC-2 activated at comparable time courses from a holding potential of 0 mV or after this series of prepulses (Fig. 2c).

These experiments demonstrate that current responses of cells expressing ClC-1–ClC-2 hetero-dimeric channels do not result from mere superpositions of currents conducted by homo-dimeric ClC-1 and ClC-2. We conclude that hetero-dimerization results in the formation of channels with novel gating properties.

Single channel recordings reveal ClC-1–ClC-2 unitary currents with only one conductance state

Macroscopic currents by ClC-1–ClC-2 hetero-dimers exhibit a significant conductance at positive voltages (Fig. 1b and c).

This is a specific property of hetero-dimeric channels, since homo-dimeric ClC-1 as well as ClC-2 currents are pronouncedly inwardly rectifying [9, 16, 20, 31]. For homo-dimeric ClC-1, rectification is based on a pronouncedly voltage-dependent unitary conductance (Supplemental Fig. 2) [8, 33]. In contrast, homo-dimeric ClC-2 single channels exhibit a constant conductance; however, there is no macroscopic outward current since all channels are closed at positive potentials [20, 38].

We performed single channel recordings to identify the unitary events underlying outward current by hetero-dimeric channels. For these experiments we used a cell line that expresses the hetero-concatameric construct in a tetracycline inducible manner and thus allows a tight control of channel density in the plasma membrane. As homo-dimeric channels from the CLC family exhibit two identical conduction pathways, "double-barreled" channels with two subconductance states are usually obtained in single channel recordings [19, 30, 36, 38]. We observed only one conductance state in recordings from ClC-1–ClC-2 heteroconcatamers, with current amplitudes similar at both voltages (Fig. 3a and b; 0.18 ± 0.01 pA at -100 mV, $n=10$; 0.17 ± 0.02 pA at $+100$ mV, $n=13$; $P=0.57$). Single channel recordings from the same inside-out patch revealed higher activity and thus open probabilities at -100 mV relative to $+100$ mV. This behavior nicely corresponds to the hyperpolarization-induced activation in macroscopic recordings. However, because of the low absolute number of open events it was impossible to accurately count the number of channels within the membrane patch, and we could therefore not determine absolute open probabilities.

The single conductance state in ClC-1–ClC-2 hetero-dimers might either be conducted by the ClC-1 or the ClC-2 protopore. The indistinguishable single channel amplitudes at positive and at negative voltages follow the voltage-independent conductance of homo-dimeric ClC-2. We therefore conclude that the protopore observed in single channel recordings on ClC-1–ClC-2 hetero-dimers likely represents an altered ClC-2 protopore. However, single-channel current amplitudes of ClC-1–ClC-2 hetero-dimers differ from reported amplitudes for homo-dimeric ClC-2 (Fig. 3c and d; -0.23 ± 0.02 pA at -100 mV [38], $n=6$, $P=6 \times 10^{-4}$) as well as for homo-dimeric ClC-1 (Fig. 3e and f; -0.13 pA± 0.01 pA at -100 mV [41], $n=5$, $P=0.02$).

We might have missed single ClC-1 protopore currents because of their small unitary current amplitude. However, earlier experiments have demonstrated that single channel recordings are feasible also for WT ClC-1 [36, 41], and we successfully repeated such experiments in this study (Fig. 3e and f). We thus conclude that the ClC-1 protopore of the hetero-concatamer must be closed under steady-state conditions. Experiments which repeated the protocols for macroscopic currents in Fig. 2a to test a putative second protopore did not unambiguously reveal

a second conductance state, most likely because capacitative artifacts and the low open probability of ClC-1–ClC-2 channels masked short events of the fast deactivating process.

Taken together, these experiments indicate that hetero-dimerization affects gating and also anion conduction of individual protopores.

Separation of ClC-1 and ClC-2 protopores by 9-anthracene carboxylic acid

Single channel recordings suggest that the ClC-2 protopore carries most of the steady-state currents in macroscopic recordings. To further verify this assignment we used 9-anthracene carboxylic acid (9-AC) which blocks CLC channels by binding within the ion conduction pathway at different K_Ds for homo-dimeric ClC-1 (13 μM) and ClC-2 (620 μM) [13].

Figure 4a shows current responses from a cell expressing the ClC-1-ClC-2 hetero-dimer upon perfusion with solutions containing either 125 or 500 μM of 9-AC. Currents through ClC-1 as well as through ClC-2 protopores were elicited by repetitive voltage steps to -140 mV interrupted by a short 10 ms pulse to $+200$ mV. Whereas the transient deactivating current component upon the voltage step back to -140 mV was completely blocked at 125 μM 9-AC, steady-state currents at negative and at positive potentials were little affected by this concentration. Even a concentration of 500 μM 9-AC was not sufficient to completely block this current component. Figure 4b depicts the time course of the transient deactivating current component (filled circles) as well as of the steady-state current component (open circles) versus the time after application of 9-AC and during the wash-out of the compound. Because of the different dissociation constants blocking kinetics were studied at a 9-AC concentration of either 125 μm for the transient current or 500 μM for the steady-state current component (Fig. 4b). K_D values were calculated individually and—for the transient deactivating current component—found to be similar to homo-dimeric ClC-1 ($K_D=14 \pm 3$ μM, $n=7$) and—for the steady-state current amplitude—to be similar to homo-dimeric ClC-2 ($K_D=452 \pm 59$ μM, $n=6$). Furthermore, most of the current at positive potentials seems to be carried by the ClC-2 protopore as a significant reduction in amplitude at $+200$ mV was only observed upon application of the higher concentration of 9-AC.

To exclude effects of concatenating subunits on the affinity towards 9-AC, we also determined K_D values for the homo-concatameric ClC-1–ClC-1 construct for the same voltage protocol yielding indistinguishable values (Supplemental Fig. 3; $K_D=13 \pm 1$ μM, $n=5$; $P=0.45$). The pharmacological block using 9-AC therefore assigns steady-state currents upon hyperpolarization and at positive potentials to the ClC-2 and the transient current component upon stepping back to

Fig. 3 Single channels recordings display a single conductance level of ClC-1–ClC-2 hetero-concatamers with amplitudes between values for homo-dimeric ClC-1 and ClC-2. **a** Representative 3.4 s window from single channel recordings of two different patches containing most likely more than one ClC-1–ClC-2 hetero-concatamer. **b** Amplitude histograms of the recordings shown in **a** indicate a single conductance level at ~0.2 pA at negative and positive potentials. **c** Representative single channel recording from one patch containing a single ClC-2 channel at −100 or +100 mV. **d** Amplitude histograms corresponding to the recordings shown indicating a two conductance levels at ~0.24 and ~0.48 pA at −100 mV while showing no activity at positive potentials. **e** Representative 1 s window from a single channel recording of one patch containing most likely two ClC-1 channels at −100 or +50 mV. **f** Amplitude histograms from the full recording time from the recording shown in **e**
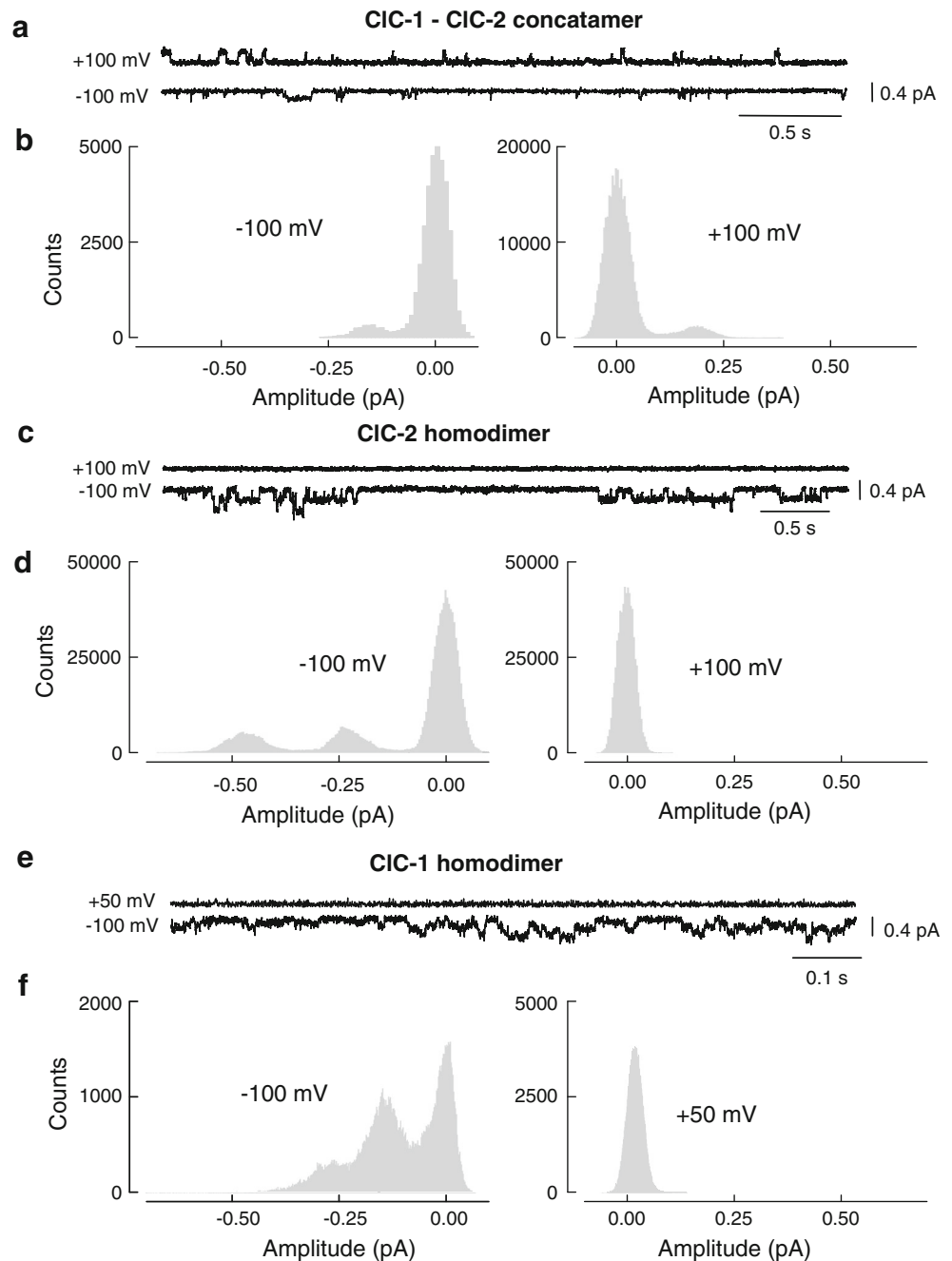
−140 mV from the short voltage step to +200 mV to the ClC-1 protopore.

Gating of the ClC-1 protopore

We next compared kinetic properties of the deactivating current component with homo-dimeric ClC-1 channels. We took advantage of the distinct time and voltage dependences of ClC-1 and ClC-2 to separate fast gating of the ClC-1 protopore from other gating processes of hetero-dimeric channels (Fig. 5a). The protopore gate of homo-dimeric ClC-1 channels exhibit time constants between 0.1 ms at positive and 10 ms at negative voltages [1, 23], as compared to values between 10 and 50 ms in WT ClC-2 channels [20, 38]. A hyperpolarizing conditioning pulse to open the slow gate allows observation of protopore opening and closing by the fast gate. To separate fast gates of the ClC-1 and ClC-2 protopores, short (2 ms) interpulses to variable voltages were inserted. To obtain the fast gate activation curve of the ClC-1 protopore the deactivating current component at a consecutive step to −120 mV was plotted against the prepulse potential (Fig. 5b). Since measured current amplitudes represent sums

Fig. 4 9-Anthracene carboxylic acid blocks the ClC-1 and ClC-2 protopore with different affinity. **a** Voltage protocol and representative current responses in the presence of 0, 125, or 500 μM 9-AC. **b** Representative time courses of the normalized transient deactivating current component (*filled symbol*) upon application of 125 μM 9-AC and the subsequent wash-out phase, and of the normalized steady-state current (*open symbol*) at −140 mV upon and after application of 500 μM 9-AC
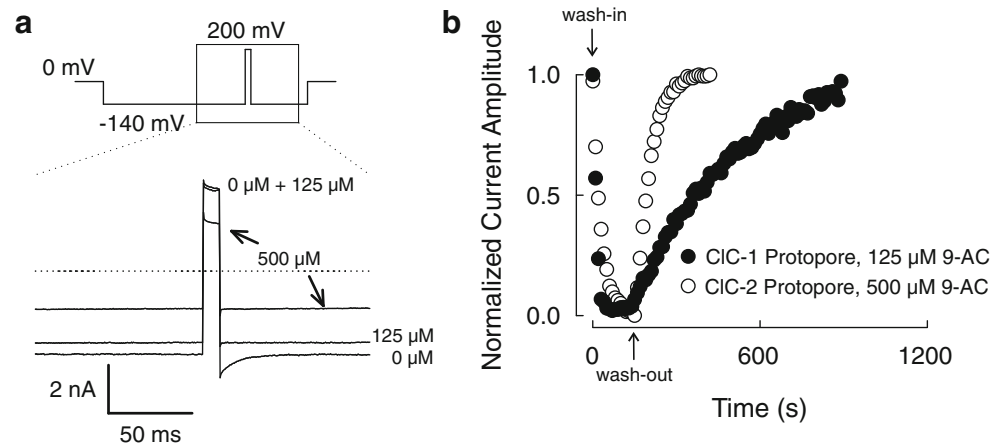
of ClC-1 and ClC-2 current components this plot only provides changes of the relative open probability with voltage.

Separation of ClC-1 and ClC-2 requires that voltages steps are short enough to prevent large changes of the open probability of the ClC-2 protopore. This restriction leads to prepulse durations that were not long enough to allow determination of steady-state activation of the ClC-1 fast gate at all voltages. To allow a comparison of fast gate activation in homo- and hetero-dimeric channels, we additionally determined activation curves of WT ClC-1 channels with the same pulse protocol used for hetero-dimeric channels. Voltage dependences of fast activation in homo- and hetero-dimeric channels were compared at three external [Cl⁻], as fast activation depends on the extracellular [Cl⁻] [33]. For [Cl⁻]$_o$ of 1 and 10 mM, ClC-1 protopores showed identical behavior in homo- and hetero-dimeric assemblies (Fig. 5b, Table 1). For [Cl⁻]$_o$ of 150 mM, the activation curve of WT channels is slightly less steep than the corresponding curve of hetero-dimeric channels. This difference is most likely due to the fact that slow gating of WT channels is faster than in hetero-dimeric channels, so that the slow gate might already incompletely activate or deactivate during the short pulses used. The kinetic analysis further supported the notion that the deactivating current component of hetero-dimer currents is conducted by the ClC-1 protopore.

To determine the voltage dependence of slow activation of the ClC-1 protopore we measured current responses to long steps of variable potentials that were interrupted by a 2-ms step to +200 mV (Fig. 5c). Since the absolute open probability of the fast gate of ClC-1 changes during the short interpulse to a constant value above zero [23], the amplitude of the deactivating current component (ΔI) after the depolarizing step (Fig. 5c, arrow) depends on the steady-state fast gate open probability at the test potential as well as on the open probability of the slow gate. Assuming independence of fast and slow gates, ΔI is a function of the open probabilities, the

number of channels and the unitary current amplitude normalized by the unitary conductance as described in Eq. 5 in the "Methods" section. This calculation provides a voltage dependence of slow gate activation curve that is inverted and shifted towards more negative values relative to the values from homo-dimeric ClC-1 (Fig. 5d).

We conclude that hetero-dimerization leaves fast protopore gating of ClC-1 unaltered, but changes the voltage dependence and kinetics of slow gating.

Gating of the ClC-2 protopore

To describe gating of the ClC-2 protopore within the hetero-dimeric assembly without interference by a pharmacological compound such as 9-AC, we took advantage of the distinct rectification of currents through ClC-1 and ClC-2 protopores. Homo-dimeric ClC-1 is inwardly rectifying with nearly zero conductance at voltage positive to +100 mV [18, 24]. Although open channel rectification was suggested to be the basis of inward rectification of macroscopic ClC-1 currents [8, 34], this has not been unambiguously demonstrated experimentally. We used noise analysis to accurately determine the absolute number of channels by non-stationary noise analysis at −155 mV (Supplemental Fig. 2a). The number of channels was then used together with the steady state variance of macroscopic currents above −80 mV to determine single channel amplitudes between −80 and +100 mV (Supplemental Fig. 2b). Our results demonstrate that the unitary conductance changes with voltage and that this voltage dependence fully accounts for the observed macroscopic inward rectification in WT ClC-1 (Supplemental Fig. 2c).

WT ClC-2 exhibits a linear unitary current–voltage relationship resulting in more than tenfold larger current amplitudes at +200 mV than the corresponding value of ClC-1 [20, 38]. A plot of the instantaneous current amplitude at a test step to +200 mV following steps to variable voltages therefore

provides the voltage dependence of the open probability of ClC-2 protopores in isolation.

Figure 6 gives pulse protocols to determine fast and slow activation curves of the ClC-2 protopore of ClC-1–ClC-2 hetero-dimeric channels. Cells were subjected to 500 ms steps to varying voltages between −140 and +100 mV followed by a 5 ms step to +200 mV (Fig. 6a, top). Currents at +200 mV were normalized and plotted versus the preceding voltage, providing the voltage dependence of the relative open probability of the ClC-2 protopore. ClC-2 protopore activation curves can be fit with Boltzmann distributions (Fig. 6c, Table 2).

We then separated fast and slow gating using the method developed by Accardi and Pusch [2, 20]. Assuming that fast and slow gating are independent of each other, the probability of the channel to be open (Po) is the product of the open probabilities of both gates. Fast gating is one order of magnitude faster than slow gating so both can be separated temporally (Fig. 6b). To measure the relative open probability of the slow gate (P_{slow}) in isolation, a short (15 ms) pulse that activates the fast gate was inserted prior to the test step in the voltage protocol to measure open probabilities (Fig. 6a, bottom). The duration of the test pulse was chosen to be identical as in experiments separating fast and slow gating of homo-dimeric channels [9, 20]. The relative open probability of the fast gate (P_{fast}) was calculated as the ratio of relative open probabilities of the channel to the relative slow gate open probability (Fig. 6c). Open probabilities were then fit by a Boltzmann equation resulting in half maximal activation points for P_{slow} and P_{fast}. The voltage dependence of fast as well as of slow activation of the ClC-2 protopore is shifted in hetero-dimeric channels to more positive potentials as compared to homo-dimeric ClC-2 (Table 2). Moreover, hetero-dimerization results in a minimal open probability of the fast gate (Fig. 6c) clearly above zero. This result is in full agreement with the single channel activity observed in unitary current measurements on ClC-1–ClC-2 hetero-dimers (Fig. 3).

Taken together, these experiments demonstrate that fast as well as slow gating of ClC-2 protopores is altered in ClC-1–ClC-2 hetero-dimers as compared to ClC-2 homo-dimers.

ClC-1 and ClC-2 protopores differ in the voltage dependence and kinetics of slow gating in hetero-dimeric assemblies

The analyses presented in Figs. 4 and 5 permit a direct comparison of ClC-1 and ClC-2 slow gating in hetero-concatameric channels (Fig. 7a). Slow gating of ClC-1 and ClC-2 protopores differs in voltage dependence and in absolute open probabilities. Whereas the ClC-1 protopore slow gate is closed at positive potentials (Fig. 2), the ClC-2 slow gate must be open to permit the observed single channel activity (Fig. 3a). Moreover, the voltage dependence of slow

Fig. 5 Fast and slow gating of the ClC-1 protopore of ClC-1–ClC-2 hetero-dimeric channels. **a** Representative current traces and pulse protocols used to calculate the relative open probability of the fast gate of ClC-1. **b** Voltage-dependencies of the relative fast gate open probabilities of ClC-1 protopores for three different external [Cl⁻]. *Continuous lines* give fits to Boltzmann functions, and *dashed lines* give responses from homo-dimeric ClC-1 currents to the same conditions. **c** Representative current traces and pulse protocols used to calculate the relative open probability of the slow gate of ClC-1 and fast gate deactivation time constants. **d** Voltage dependence of the ClC-1 slow gate activation in ClC-1–ClC-2 hetero-dimeric channels. The *dashed line* corresponds to slow gate open probabilities from homo-dimeric ClC-1 channels

Table 1 Midpoint of activation of fast ClC-1 gating for ClC-1 homo-dimeric and ClC-1–ClC-2 hetero-dimeric channels

	150 mM [Cl⁻] (mV)	10 mM [Cl⁻] (mV)	1 mM [Cl⁻] (mV)
hClC-1 homodimer	-29.0 ± 3.1 $n=4$	$+28.4\pm4.5$ $n=4$	$+64.1\pm2.6$ $n=3$
hClC-1/hClC-2 concatamer	-29.1 ± 2.5 $n=11$	$+27.4\pm2.8$ $n=4$	$+69.2\pm2.4$ $n=5$

activation of the ClC-1 protopore is shifted to negative potentials compared to the ClC-2 pore.

We used an envelope pulse protocol to separate the time courses of slow gating of ClC-1 and ClC-2 protopores (Fig. 7b). Cells were hyperpolarized at the desired voltage for various durations before being interrupted by a short pulse to +200 mV and the return to the preceding voltage. The number of open ClC-2 protopores was measured as the current at +200 mV, whereas ClC-1 activation was measured as the amplitude of the deactivating component (Δ) following the constant activation of the fast gate at +200 mV. A plot of these values versus the preceding pulse duration provides the time dependence of activation of ClC-1 and ClC-2 protopores in separation. Fitting a monoexponential functions provides slow time constants for the activation of either ClC-1 or ClC-2 protopores with significantly different values across all voltages studied (Fig. 7c and d, Table 3).

Our results suggest that hetero-dimerization abolishes common gating and results in separate slow gating processes of individual ClC-1 and ClC-2 protopores.

Discussion

CLC channels and transporters are dimeric proteins with two largely independent subunits. This concept was originally based on the occurrence of two equally spaced and independently gated conductance states in single channel recordings of ClC-0 [29, 30]. The generation of artificial monomers of the prokaryotic transporter ecClC that fulfill normal transport functions provided additional proof of this concept [32]. However, there are functional interactions between the two subunits of a functional CLC channel or transporter. Single channel recordings of CLC channels show joint opening and closings of both protopores [19, 30, 36, 38], a behavior that is currently interpreted by a common gate that opens and closes both protopores together. Processes that gate individual protopores are usually assumed not to interact with each other [30].

To further characterize functional interactions between the two subunits during individual and common gating processes
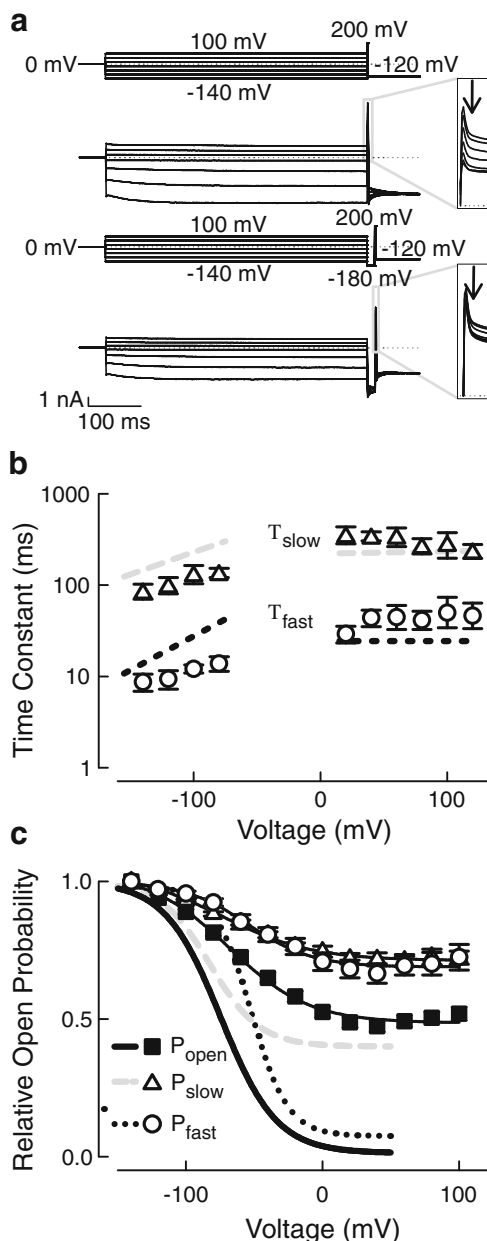
Fig. 6 Fast and slow gating of the ClC-2 protopore of ClC-1–ClC-2 hetero-dimeric channels. **a** Representative current traces and pulse protocols used to calculate the relative open probability and the relative open probabilities of the fast gate and the slow gate (*arrows*) of ClC-2. **b** Time constants of the activation (negative voltages) and deactivation (positive voltages) kinetics of ClC-2 protopore currents obtained by bi-exponential fits. Fast time constants were determined in the presence of 0.1 mM 9-AC to block possible interference by the ClC-1 protopore. **c** Voltage dependencies of the relative combined as well as the separated fast and slow gate open probabilities of ClC-2. *Lines without symbols* show respective homodimeric ClC-2 open probabilities (*solid line* overall open probabilities; *dotted line* fast gate; *dashed line* slow gate)

we performed single channel and whole cell patch clamp recordings on hetero-dimeric ClC-1–ClC-2 channels. We generated a concatameric construct to express covalently linked hetero-dimeric channels in mammalian cells without visible

Table 2 Gating parameters of ClC-2 protopores for ClC-2 homo-dimeric and ClC-1–ClC-2 concatameric channels

	Overall (mV)	Fast gate (mV)	Slow gate (mV)
hClC-2 homodimer	−82.9±3.1 *n*=7	−61.3±3.9 *n*=6	−91.8±5.3 *n*=5
hClC-1/hClC-2 concatamer	−66.8±1.8 *n*=6	−51.6±3.9 *n*=6	−74.4±5.3 *n*=6

Midpoints of activation were determined by Boltzmann fits to the voltage dependence of relative open probabilities

formation of ClC-1 or ClC-2 monomers (Fig. 1a). This maneuver resulted in macroscopic currents that activated upon hyperpolarization and exhibited a significant conductance at positive potentials unlike a superposition of homo-dimeric currents (Fig. 2). A significant conductance at positive potentials was also observed for spontaneously formed ClC-1–ClC-2 hetero-dimers [28] suggesting close functional similarity between spontaneous and covalently linked hetero-dimers. In single-channel recordings from cells expressing the concatameric constructs, we observed single channels with only a single conductance state (Fig. 3). The voltage-independent conductance as well as the gating properties of these unitary events resembled homo-dimeric ClC-2 single

channels and were thus assigned to the ClC-2 protopore within the hetero-dimeric assembly. This assignment was further supported by experiments with 9-AC that revealed similar affinity for steady-state currents and for homo-dimeric ClC-2 that differed significantly from transient deactivating currents and homo-dimeric ClC-1 (Fig. 4, Supplemental Fig. 3). We were unable to observe another conductance state in single channel recordings in agreement with the ClC-1 protopore being closed at steady-state conditions.

The unitary current amplitudes in ClC-1–ClC-2 are between values of homo-dimeric ClC-1 and ClC-2 channels [23, 31, 36, 38, 41]. This finding is surprising since structural data suggest two separate conduction pathways that are not in close spatial proximity. Weinberger at al. recently demonstrated reduced current amplitudes in C277Y ClC-1 channels [41]. C277 is close to the dimer interface and has been implied to play a role in common gating of CLC channels. It is located far away from the conduction pathway [1, 27]. It is conceivable that small changes in the electrostatic environment following dimerization can lead to rearrangements of amino acid side chains across the extensive interface between the two halves of CLC channels. Taken together, our result suggests that interactions between the two subunits can modify ion conduction also in CLC homo-dimers. In earlier studies on ClC-0–ClC-1 or ClC-0–ClC-2 concatenated hetero-dimers [42], no

Fig. 7 Slow gating of ClC-1 and ClC-2 protopores in ClC-1–ClC-2 hetero-dimeric channels. **a** Relative slow open probabilities for ClC-1 and ClC-2 protopores differ in voltage dependence. **b** Representative current traces used to determine slow activation time courses of ClC-1 and ClC-2 protopores in hetero-dimeric channels. Cells were hyperpolarized to various potentials for increasing durations followed by a short depolarization to +200 mV. **c** Normalized current amplitudes from representative experiments demonstrate the different slow activation time courses for ClC-1 and ClC-2 subunits. **d** Comparison of slow time constants for each protopore with the corresponding homodimer data
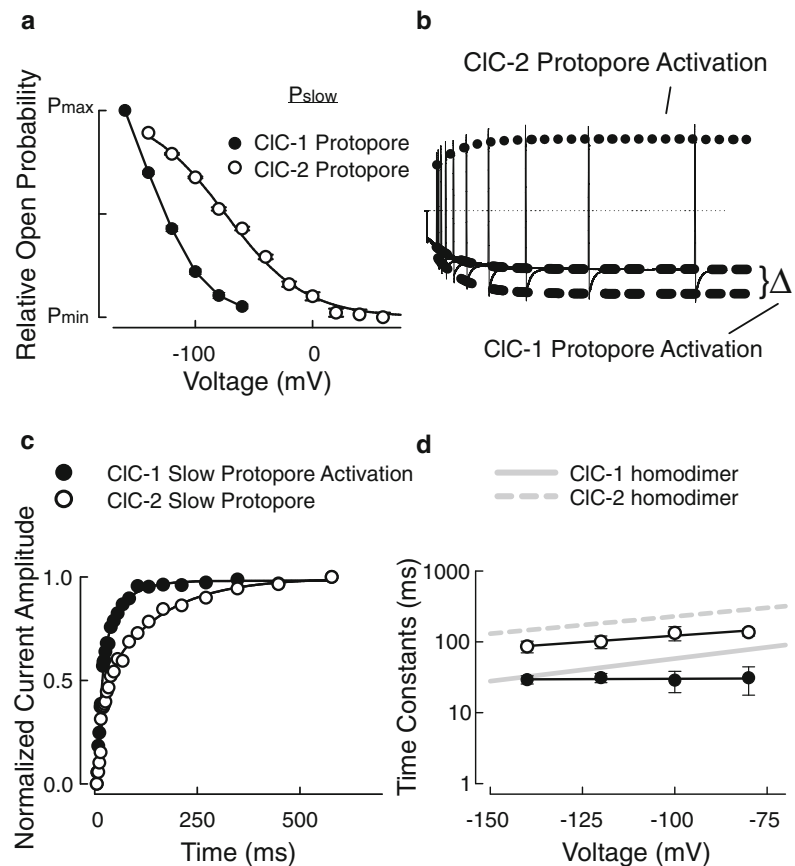
Table 3 Slow time constants of ClC-1 protopore and ClC-2 protopore activation in hetero-concatameric channels as determined by a bi-exponential fit to data from envelope protocols

Voltage (mV)	ClC-1 protopore Slow time constant (ms)	ClC-2 protopore Slow time constant (ms)	P value
−80	31.08±13.40 (n=3)	111.34±8.68 (n=4)	<0.01
−100	28.74±9.61 (n=5)	102.44±6.38 (n=5)	<0.01
−120	31.14±4.61 (n=5)	70.46±5.83 (n=5)	<0.01
−140	29.24±3.87 (n=6)	64.35±7.06 (n=6)	<0.01

changes in unitary current amplitudes of the protopores were observed, indicating isoform-specific variation in this particular property.

In addition to the effects on conductance, single channel recordings on ClC-1–ClC-2 show activity at +100 mV, whereas homo-dimeric ClC-2 channels are fully closed by the fast protopore gate at positive voltages [20, 38]. Activation curves of the ClC-2 pore were shifted to more positive potentials as compared to homo-dimeric assemblies and differed in voltage dependence (Fig. 6). Hetero-dimerization thus alters two functional properties of individual protopores, ion conduction, and individual gating.

Fast gating of the ClC-1 protopore turned out to be similar in both homo- and hetero-dimeric channels (Fig. 5). We determined fast activation and deactivation time constants and midpoints of activation for three different external [Cl⁻], without significant differences between WT ClC-1 and hetero-dimeric assemblies. In contrast to the lack of effects on fast gating, the adjacent ClC-2 protopore has dramatic effects on slow gating of the ClC-1 pore. In ClC-1–ClC-2 hetero-dimers, the ClC-1 protopore can only be activated if the membrane is hyperpolarized previously (Figs. 2 and 5). We conclude that hetero-dimerization of ClC-1 and ClC-2 results in the formation of a novel slow hyperpolarization-activated gate that has to be open to permit current flow through the ClC-1 protopore. The absence of any fast activation of ClC-1 without prior activation of this particular slow gate indicates that this gate of ClC-1 is closed at positive voltages (Fig. 5).

At first glance, slow activation of the ClC-1 current component (Fig. 2) could be interpreted as common gating upon hyperpolarizing voltage steps. However, whereas slow gating keeps the ClC-1 protopore closed at positive potentials, ClC-2 protopores are active at these potentials under steady-state conditions. Moreover, slow gating of the ClC-1 and the ClC-2 protopores differ in their voltage dependence as indicated by the significantly shifted half-maximal activation and in slow gate time constants (Fig. 7). We conclude that distinct slow gates must act on each protopore separately in hetero-dimeric ClC-1–ClC-2 channels (Fig. 7).

Previous studies revealed the absence of the characteristic slow gating of homo-dimeric ClC-0 in ClC-0–ClC-1 hetero-dimers [42]. The effects of protopore and common gating were not examined in detail in this study. ClC-0–ClC-1 differs from ClC-1–ClC-2 hetero-dimers in both pores being active in single channel recordings.

A recent study identified Y578 of ClC-1, corresponding to Y553 in ClC-2, as critical in the process of common gating [4]. The authors proposed that this tyrosine residue interacts with the "gating glutamate" (Glu232 in ClC-1) as the "final effector" of ClC-1 common gating. This hypothesis predicts a critical role of protopore-specific amino acid side chains in the final steps of common gating. Our results of different slow gate kinetics for two separate protopores in a hetero-dimeric channel might thus be explained by the different conformations and surroundings of those important side chains in the respective monomers. This hypothesis explains our finding of two separate "slow gates" within ClC-1–ClC-2-hetero-dimeric channels as—at least—the final molecular gate is different for each protopore.

Novel slow gating processes in mutant or hetero-dimeric channels have often been interpreted as changes in common gating [3, 40] The results on ClC-1–ClC-2 hetero-dimeric channels indicate that greater care has to be applied to assign novel gating processes to individual or common openings or closing in the future. In the evaluation of disease-causing mutations in heteromeric WT-mutant assemblies, these variants might not just cause effects on the mutant containing protopore but also on the adjacent one, not only through common gating but also on the level of individual gating and pore properties. Our results reiterate the importance of unitary current measurements in assigning individual and common gating processes to members of the CLC family.

In conclusion we have characterized gating of a hetero-dimeric concatamer of ClC-1 and ClC-2. We found that hetero-dimerization apparently resulted in abolished common gating but retained individual slow gating for each protopore. The decrease in the unitary current amplitude of the ClC-2 protopore from 0.23±0.02 pA (n=6) in homo-dimers to 0.18±0.01 pA at −100 mV (n=10; P<0.01) in hetero-dimeric channels and an open probability well above zero at positive voltages implies a pronounced interaction of CLC subunits in properties previously believed to be independent from the adjacent protopore.

References

1. Accardi A, Ferrera L, Pusch M (2001) Drastic reduction of the slow gate of human muscle chloride channel (ClC-1) by mutation C277S. J Physiol 534:745–752. doi:10.1111/j.1469-7793.2001.00745.x

2. Accardi A, Pusch M (2000) Fast and slow gating relaxations in the muscle chloride channel ClC-1. J Gen Physiol 116:433–444. doi:10.1085/jgp.116.3.433

3. Aromataris EC, Rychkov GY, Bennetts B et al (2001) Fast and slow gating of ClC-1: differential effects of 2-(4-chlorophenoxy) propionic acid and dominant negative mutations. Mol Pharmacol 60:200–208. doi:10.1124/mol.60.1.200

4. Bennetts B, Parker MW (2013) Molecular determinants of common gating of a ClC chloride channel. Nat Commun 4:2507. doi:10.1038/ncomms3507

5. Bryant SH, Morales-Aguilera A (1971) Chloride conductance in normal and myotonic muscle fibres and the action of monocarboxylic aromatic acids. J Physiol 219:367–383

6. Chen M-F, Chen T-Y (2001) Different fast-gate regulation by external Cl^- and H^+ of the muscle-type ClC chloride channels. J Gen Physiol 118:23–32. doi:10.1085/jgp.118.1.23

7. Chen TT, Klassen TL, Goldman AM et al (2013) Novel brain expression of ClC-1 chloride channels and enrichment of *CLCN1* variants in epilepsy. Neurology 80:1078–1085. doi:10.1212/WNL.0b013e31828868e7

8. Corry B, O'Mara M, Chung S-H (2004) Conduction mechanisms of chloride ions in CLC-type channels. Biophys J 86:846–860. doi:10.1016/S0006-3495(04)74160-0

9. De Santiago JA, Nehrke K, Arreola J (2005) Quantitative analysis of the voltage-dependent gating of mouse parotid ClC-2 chloride channel. J Gen Physiol 126:591–603. doi:10.1085/jgp.200509310

10. Dutzler R, Campbell EB, Cadene M et al (2002) X-ray structure of a ClC chloride channel at 3.0 A reveals the molecular basis of anion selectivity. Nature 415:287–294. doi:10.1038/415287a

11. Dutzler R, Campbell EB, MacKinnon R (2003) Gating the selectivity filter in ClC chloride channels. Science 300:108–112. doi:10.1126/science.1082708

12. Engh AM, Faraldo-Gómez JD, Maduke M (2007) The mechanism of fast-gate opening in ClC-0. J Gen Physiol 130:335–349. doi:10.1085/jgp.200709759

13. Estévez R, Schroeder BC, Accardi A et al (2003) Conservation of chloride channel structure revealed by an inhibitor binding site in ClC-1. Neuron 38:47–59. doi:10.1016/S0896-6273(03)00168-5

14. Fahlke C, Desai RR, Gillani N, George AL (2001) Residues lining the inner pore vestibule of human muscle chloride channels. J Biol Chem 276:1759–1765. doi:10.1074/jbc.M007649200

15. Fahlke C, Knittle T, Gurnett CA et al (1997) Subunit stoichiometry of human muscle chloride channels. J Gen Physiol 109:93–104. doi:10.1085/jgp.109.1.93

16. Fahlke C, Rosenbohm A, Mitrovic N et al (1996) Mechanism of voltage-dependent gating in skeletal muscle chloride channels. Biophys J 71:695–706. doi:10.1016/S0006-3495(96)79269-X

17. Fahlke C, Rüdel R (1995) Chloride currents across the membrane of mammalian skeletal muscle fibres. J Physiol 484:355–368

18. Fahlke C, Rüdel R, Mitrovic N et al (1995) An aspartic acid residue important for voltage-dependent gating of human muscle chloride channels. Neuron 15:463–472. doi:10.1016/0896-6273(95)90050-0

19. Fischer M, Janssen AGH, Fahlke C (2010) Barttin activates ClC-K channel function by modulating gating. J Am Soc Nephrol. doi:10.1681/ASN.2009121274

20. Garcia-Olivares J, Alekov A, Boroumand MR et al (2008) Gating of human ClC-2 chloride channels and regulation by carboxy-terminal domains. J Physiol 586:5325–5336. doi:10.1113/jphysiol.2008.158097

21. Gendreau S, Voswinkel S, Torres-Salazar D et al (2004) A trimeric quaternary structure is conserved in bacterial and human glutamate transporters. J Biol Chem 279:39505–39512. doi:10.1074/jbc.M408038200

22. Hebeisen S, Biela A, Giese B et al (2004) The role of the carboxyl terminus in ClC chloride channel function. J Biol Chem 279:13140–13147. doi:10.1074/jbc.M312649200

23. Hebeisen S, Fahlke C (2005) Carboxy-terminal truncations modify the outer pore vestibule of muscle chloride channels. Biophys J 89:1710–1720. doi:10.1529/biophysj.104.056093

24. Hebeisen S, Heidtmann H, Cosmelli D et al (2003) Anion permeation in human ClC-4 channels. Biophys J 84:2306–2318. doi:10.1016/S0006-3495(03)75036-X

25. Janssen AGH, Scholl U, Domeyer C et al (2009) Disease-causing dysfunctions of barttin in Bartter syndrome type IV. J Am Soc Nephrol 20:145–153. doi:10.1681/ASN.2008010102

26. Lin C-W, Chen T-Y (2000) Cysteine modification of a putative pore residue in ClC-0 implication for the pore stoichiometry of Clc chloride channels. J Gen Physiol 116:535–546. doi:10.1085/jgp.116.4.535

27. Lin Y-W, Lin C-W, Chen T-Y (1999) Elimination of the slow gating of Clc-0 chloride channel by a point mutation. J Gen Physiol 114:1–12. doi:10.1085/jgp.114.1.1

28. Lorenz C, Pusch M, Jentsch TJ (1996) Heteromultimeric CLC chloride channels with novel properties. Proc Natl Acad Sci U S A 93:13362–13366

29. Ludewig U, Pusch M, Jentsch TJ (1997) Independent gating of single pores in ClC-0 chloride channels. Biophys J 73:789–797. doi:10.1016/S0006-3495(97)78111-6

30. Miller C (1982) Open-state substructure of single chloride channels from Torpedo electroplax. Philos Trans R Soc Lond B Biol Sci 299:401–411

31. Pusch M, Steinmeyer K, Jentsch TJ (1994) Low single channel conductance of the major skeletal muscle chloride channel, ClC-1. Biophys J 66:149–152. doi:10.1016/S0006-3495(94)80753-2

32. Robertson JL, Kolmakova-Partensky L, Miller C (2010) Design, function and structure of a monomeric ClC transporter. Nature 468:844–847. doi:10.1038/nature09556

33. Rychkov GY, Pusch M, Astill DS et al (1996) Concentration and pH dependence of skeletal muscle chloride channel ClC-1. J Physiol 497(Pt 2):423–435

34. Rychkov GY, Pusch M, Roberts ML et al (1998) Permeation and block of the skeletal muscle chloride channel, ClC-1, by foreign anions. J Gen Physiol 111:653–665. doi:10.1085/jgp.111.5.653

35. Sánchez-Rodríguez JE, Santiago-Castillo JAD, Contreras-Vite JA et al (2012) Sequential interaction of chloride and proton ions with the fast gate steer the voltage-dependent gating in ClC-2 chloride channels. J Physiol 590:4239–4253. doi:10.1113/jphysiol.2012.232660

36. Saviane C, Conti F, Pusch M (1999) The muscle chloride channel ClC-1 has a double-barreled appearance that is differentially affected in dominant and recessive myotonia. J Gen Physiol 113:457–468. doi:10.1085/jgp.113.3.457

37. Scholl U, Hebeisen S, Janssen AGH et al (2006) Barttin modulates trafficking and function of ClC-K channels. Proc Natl Acad Sci U S A 103:11411–11416. doi:10.1073/pnas.0601631103

38. Stölting G, Teodorescu G, Begemann B et al (2013) Regulation of ClC-2 gating by intracellular ATP. Pflugers Arch-Eur J Physiol 465:1423–1437. doi:10.1007/s00424-013-1286-0

39. Thiemann A, Gründer S, Pusch M, Jentsch TJ (1992) A chloride channel widely expressed in epithelial and non-epithelial cells. Nature 356:57–60. doi:10.1038/356057a0

40. Warnstedt M, Sun C, Poser B et al (2002) The myotonia congenita mutation A331T confers a novel hyperpolarization-activated gate to the muscle chloride channel ClC-1. J Neurosci 22:7462–7470

41. Weinberger S, Wojciechowski D, Sternberg D et al (2012) Disease-causing mutations C277R and C277Y modify gating of human ClC-1 chloride channels in myotonia congenita. J Physiol. doi:10.1113/jphysiol.2012.232785

42. Weinreich F, Jentsch TJ (2001) Pores formed by single subunits in mixed dimers of different CLC chloride channels. J Biol Chem 276:2347–2353. doi:10.1074/jbc.M005733200

43. Zúñiga L, Niemeyer MI, Varela D et al (2004) The voltage-dependent ClC-2 chloride channel has a dual gating mechanism. J Physiol 555:671–682. doi:10.1113/jphysiol.2003.060046